

## Supporting Information

### Simple preparation and highly selective detection of silver ions using an electrochemical sensor based on sulfur-doped graphene and 3,3',5,5'-tetramethylbenzidine composite modified electrode

Yang Fu <sup>a,b,c</sup>, Yajie Yang <sup>a,b,c</sup>, Tayierjiang Tuersun <sup>a,b,c</sup>, Yuan Yu <sup>d</sup>

and Jinfang Zhi <sup>\*a,b,c</sup>

<sup>a</sup>Key Laboratory of Photochemical Conversion and Optoelectronic Materials, Technical Institute of Physics and Chemistry, Chinese Academy of Sciences, Beijing 100190, PR China

<sup>b</sup>Technical Institute of Physics and Chemistry, Chinese Academy of Sciences, Beijing 100190, PR China

<sup>c</sup>University of Chinese Academy of Sciences, Beijing 100049, PR China

<sup>d</sup>Institute of Atomic and Molecular Science, Shanxi University of Science & Technology, Xian 710021, PR China

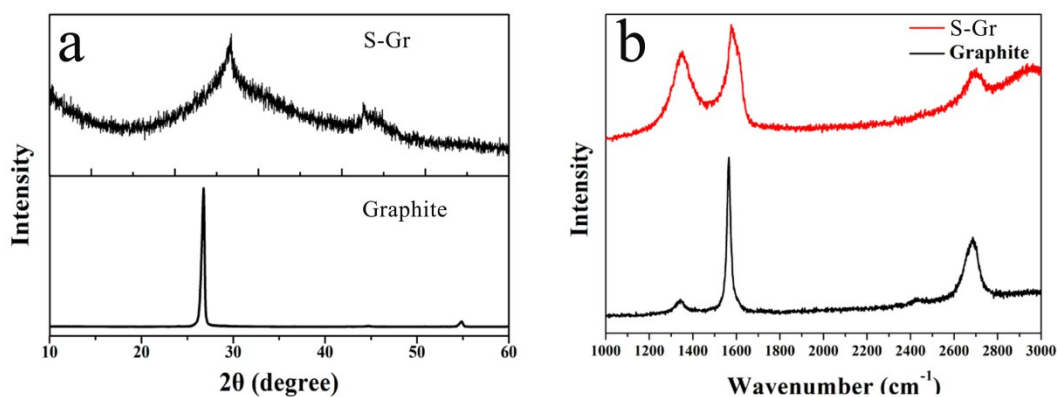


**Fig. S1** (a) XRD patterns and (b) Raman spectra of graphite and the exfoliated S-Gr.

The crystal structure of the pristine graphite and the exfoliated S-Gr were analyzed by conducting X-ray diffraction (XRD) studies in Fig. S1a. The pristine graphite exhibit a sharp peak centered at  $26.6^\circ$  and  $54.7^\circ$  corresponding to the (002) and (004) planes of graphite crystal. The exfoliated S-Gr displays a broad (002) diffraction peak due to the corrugated structure of the S-Gr and the stacked S-Gr layers. XRD result proved the successful exfoliation of graphite to producing S-Gr, which is in good agreement with the reported value.

Raman spectra of graphite and the exploited S-Gr reflect the significant structural changes from graphite to S-Gr in Fig. S1b. Two remarkable peaks in the Raman spectrum are the D band (defects) and the G band (in-plane vibration of  $sp^2$  carbon atoms). The Raman spectrum of the graphite in Fig. S1b displays a prominent G peak at  $1600\text{ cm}^{-1}$  corresponding to the first-order scattering of the  $E_{2g}$  vibration mode. The Raman spectrum of the exfoliated Gr shows that the G band is broadened and the peak of D band is present at  $1370\text{ cm}^{-1}$ . The ratio of  $I_D/I_G$  corresponds to the number of defects in graphene. The intensity of G band is higher than that of D band for the exfoliated S-Gr, thus, the ratio of  $I_D/I_G$  is less than 1, which is much lower than that of chemically or thermally reduced graphene oxide (1.2–1.5).

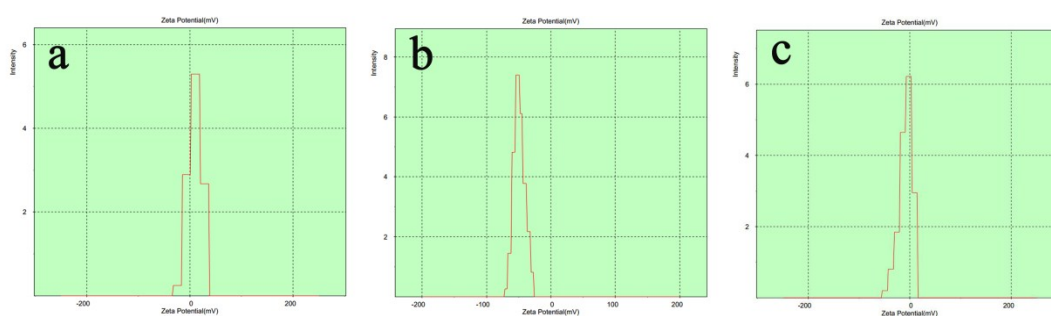


**Fig. S2** Zeta potential of (a) TMB, (b) S-Gr and c. S-Gr-TMB.

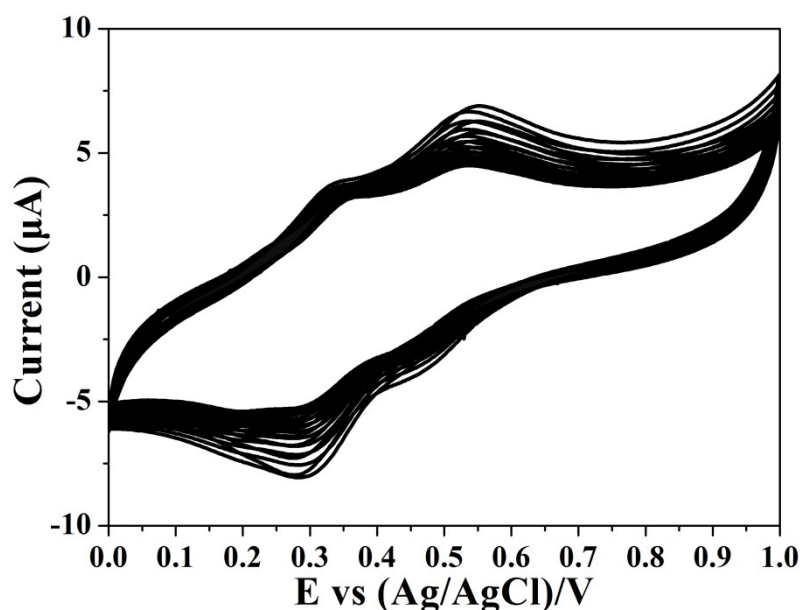


**Fig. S3** Continuous CVs of Gr-TMB/GCE recorded for 20 cycles in NaAc buffer solution (0.2 mol/L NaAc/HAc, pH = 4) at a scan rate of 50 mV/s.

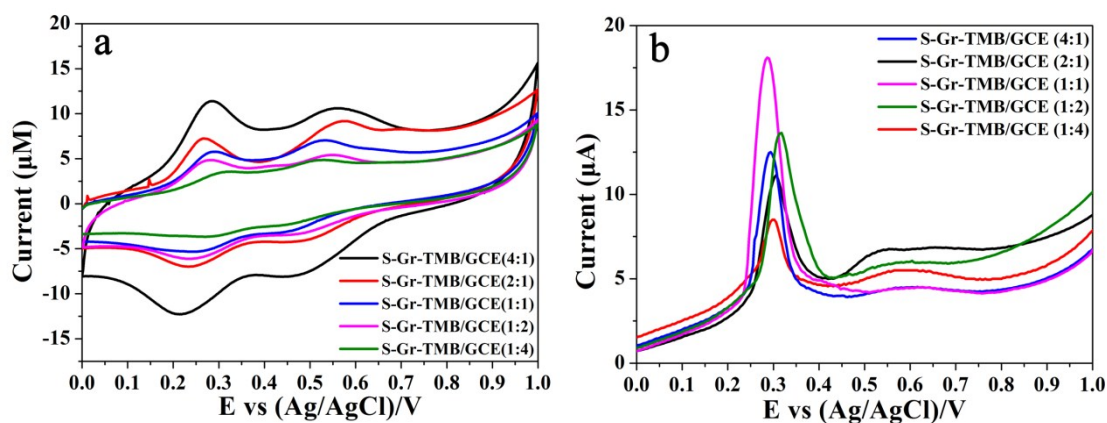


**Fig. S4** (a) CVs of the S-Gr-TMB/GCE at the five different volume ratios of S-Gr to TMB (4:1 (Black), 2:1 (Red), 1:1 (Blue), 1:2 (Pink) and 1:4 (Green)); (b) DPV scans of the S-Gr-TMB/GCE at the five different volume ratios of S-Gr to TMB (4:1 (Blue), 2:1 (Black), 1:1 (Pink), 1:2 (Green) and 1:4 (Red)).

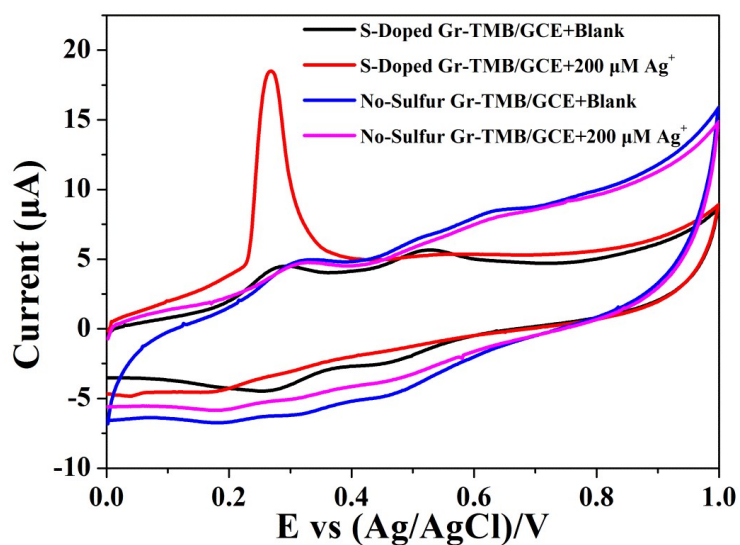


**Fig. S5** CVs of S-Gr-TMB/GCE without (Black) and with the presence of 200 μmol/L Ag<sup>+</sup> (Red), Gr-TMB/GCE without (Blue) and with the presence of 200 μmol/L Ag<sup>+</sup> (Pink).

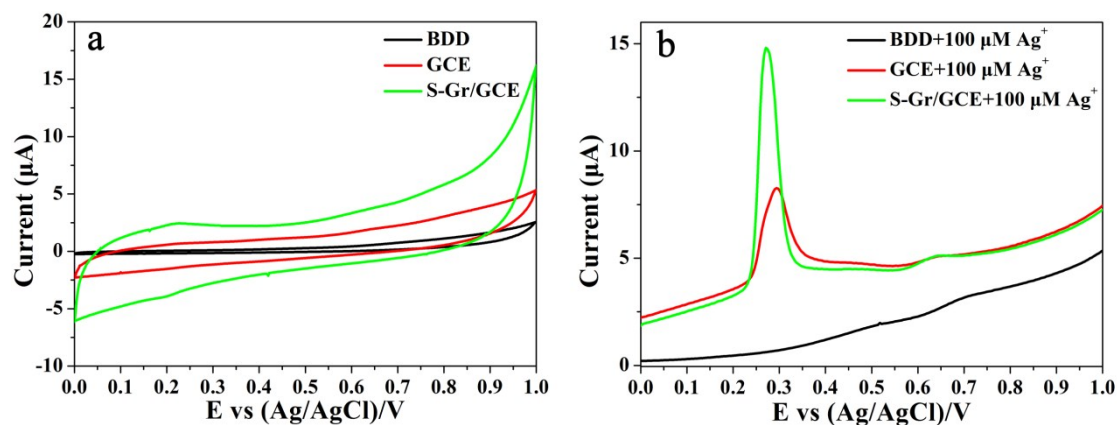


**Fig. S6** (a) CVs of BDD (Black), GCE (Red) and S-Gr/GCE (Green) in NaAc buffer solution (0.2 M NaAc/HAc, pH = 4); (b) DPV scans of BDD (Black), GCE (Red) and S-Gr/GCE (Green) with the presence of 100 μM Ag<sup>+</sup>.

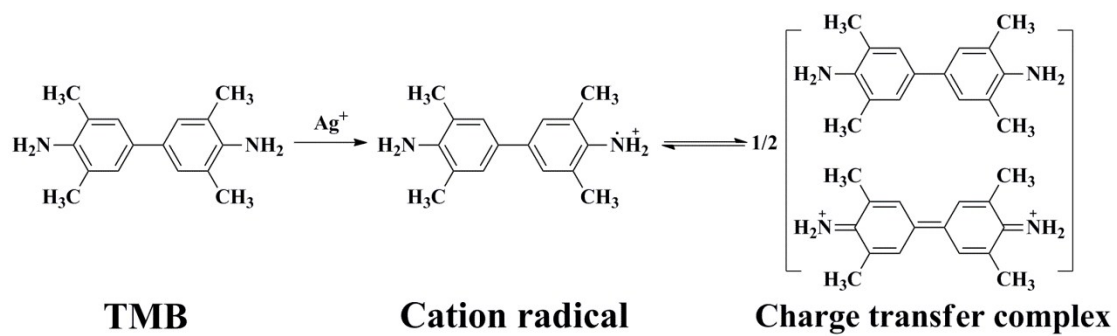


**Fig. S7** The coordination scheme of  $\text{Ag}^+$  to TMB.